

Exact solutions of the generalized Navier–Stokes equations for benchmarking

Andrei Bourchtein^{*,†}

Department of Mathematics, Pelotas State University, Campus Universitario da UFPel, 96010-900, Brazil

SUMMARY

The generalized Navier–Stokes equations for incompressible viscous flows through isotropic granular porous medium are studied. Some analytical classic solutions of the Navier–Stokes equations are generalized to the case of the considered equations. Obtained solutions of generalized equations reduce to classic ones as porosity effect disappears. Average velocity of generalized solutions is calculated and evaluated in two limiting regimes of flow. In the shallow conduit, the generalized flow rate approximates the free (without porous medium) flow rate and in the case of removed boundaries this approaches Darcy’s law. The use of the derived exact solutions for benchmarking purposes is described. Copyright © 2002 John Wiley & Sons, Ltd.

KEY WORDS: porous medium; generalized Navier–Stokes equations; analytical solutions; benchmarking problems

1. INTRODUCTION

Due to the non-linearity of the Navier–Stokes equations only a small number of exact solutions have been found. The most recent reviews of analytical solutions of the Navier–Stokes equations and its classification were given by Wang [1, 2]. These solutions are important because they represent some fundamental fluid flows and serve for checking the accuracy of approximate methods, in particularly, numerical schemes. There are three traditional methods of verifying numerical schemes and solutions in computational fluid dynamics: the exact solutions, experimental data sets and ‘exact, benchmarking’ high-resolution numerical simulations. The importance of one of these modes increases when others are not accessible or have a shortage of data. This is the case of hydrodynamic models in porous media. We consider one model of laminar flow through a granular porous medium which can be represented in the form of the generalized Navier–Stokes equations. Therefore, it is useful to generalize

* Correspondence to: A. Bourchtein, Rua Anchieta 4715, bloco K, ap. 304, 96020-250 Pelotas, Brazil.

† E-mail: burstein@conex.com.br

Contract/grant sponsor: Brazilian Foundation; contract/grant number: FAPERGS 01/60053.9

some known analytical solutions of the Navier–Stokes equations to the case of the considered model. We think this is in itself an interesting problem. Also these solutions can be used to verify the validity of the differential model because in some simple cases they can be compared with known experimental data of average characteristics of flows and with empirical laws such as Darcy’s law. Finally, these solutions can be used for benchmarking of numerical schemes based on the considered or similar models.

The generalized Navier–Stokes equations applied to a description of incompressible viscous laminar flow through a rigid isotropic granular porous medium have been considered by different authors (for example, References [3–5]). We follow the paper by DuPlessis and Masliyah [5]. The advantages of their model are its applicability to granular porous media over the entire porosity range and its simple adaptability to numerical simulations. The primitive equations have the following form:

$$\rho \mathbf{V}_t + \rho(\mathbf{V} \cdot \nabla) \frac{\mathbf{V}}{n} = -n \nabla p + \mu \nabla^2 \mathbf{V} - \mu F \mathbf{V} - n \rho \mathbf{g}, \quad \nabla \cdot \mathbf{V} = 0 \quad (1)$$

Here, the common denotations are used for fluid and porous medium characteristics: \mathbf{V} is a fluid velocity vector, p is a pressure; \mathbf{g} is the gravitational force. The fluid is specified by definition of density ρ and dynamic viscosity μ . The characteristics of porous medium are porosity n and porosity function F . Porosity n is defined as a ratio of volume of the void space to the bulk volume of a porous medium and it changes from zero to one ($n \in (0, 1]$). Function F represents an additional drag force which describes influence of porous medium on flow. This function depends on porosity n only, it is continuous, decreasing and positive on interval $(0, 1]$, F becomes infinite as n approaches zero and tends to 0 as n approaches 1. Comparing this system with usual incompressible Navier–Stokes equations one can see that the latter is the particular case of the model (1) when $n = 1$. In the subsequent sections, we will derive some particular solutions of Equation (1) assuming that dynamic viscosity μ and porosity n are constants.

Considering the primitive system in 4D domain $[0, T] \times \bar{\Omega}$, where $\bar{\Omega} = \Omega + \partial\Omega$ is a 3D spatial bounded domain with boundary $\Gamma = \partial\Omega$, we have to specify the initial and boundary conditions to define the unique solution:

$$\mathbf{V} = \mathbf{V}_0 \quad \text{on } \bar{\Omega} \quad \text{at } t = 0 \quad (2)$$

(initial condition, \mathbf{V}_0 is the given function of spatial variables),

$$\mathbf{V} = \mathbf{V}_\Gamma \quad \text{on } \Gamma = \partial\Omega \quad \text{for all } t \in [0, T] \quad (3)$$

(no-slip boundary condition, \mathbf{V}_Γ is the given function of the time variable and two spatial variables).

These conditions have to subject to some constraints such as initial divergence condition

$$\nabla \cdot \mathbf{V}_0 = 0 \quad \text{on } \Omega$$

integral divergence condition

$$\int_{\Gamma} \mathbf{V}_\Gamma \cdot \mathbf{n} d\Gamma = 0 \quad \text{for all } t \in [0, T]$$

and agreement condition between initial and boundary conditions $\mathbf{V}_0 = \mathbf{V}_\Gamma$ on Γ at $t = 0$ [6, 7]. We assume that the last constraints are satisfied by appropriate choice of initial and boundary conditions and then we will not mention these conditions anymore.

2. COUETTE-POISEUILLE FLOW

First, we will generalize the Couette–Poiseuille flow between two parallel moving plates. We use the classic approach and introduce an inertial Cartesian system with the z -axis normal to the plates and the xy -plane lying midway between the plates so that the plates are located at planes $z = \pm h$ (see Figure 1 for problem geometry). Using the Couette–Poiseuille simplification $\mathbf{V} = \mathbf{V}(z)$ and following the classic solution deriving method, one can reduce the primitive system (1) with no-slip boundary conditions (3) to set of decoupled equations

$$\mu u_{zz} - \mu Fu = -nG = np_x, \quad \mu v_{zz} - \mu Fv = -nH = np_y, \quad p_z = -\rho g, \quad w_z = 0 \quad (4)$$

with boundary conditions

$$\mathbf{V}(-h) = \mathbf{V}_1, \quad \mathbf{V}(h) = \mathbf{V}_2 \quad (5)$$

Here, u, v, w are the velocity components, $\mathbf{V} = (u, v, w)$, $\mathbf{V}_1 = (U_1, V_1, 0)$ and $\mathbf{V}_2 = (U_2, V_2, 0)$ are the velocity of the lower and upper plates, respectively, and G and H are the separation

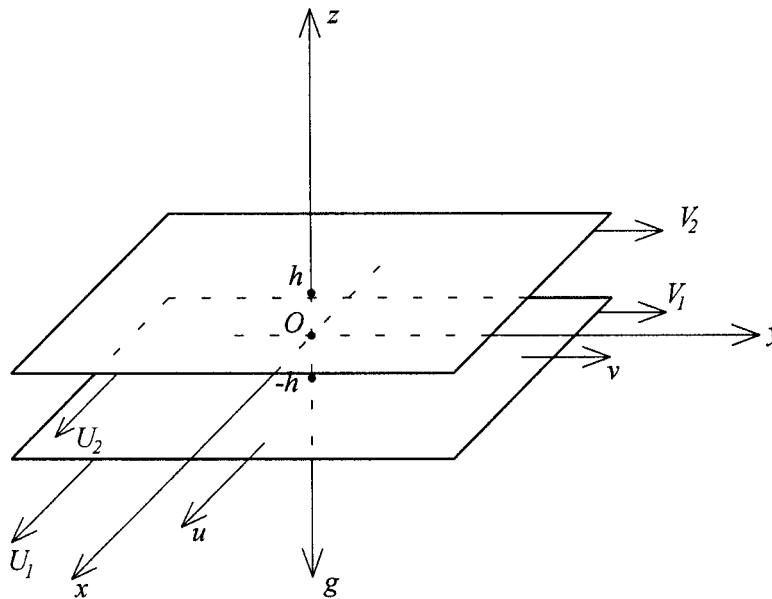


Figure 1. Geometry for Couette–Poiseuille flow.

constants. The solution of (4) and (5) has the following form:

$$u(z) = \frac{1}{\sinh(2\sqrt{F}h)} [U_1 \sinh(\sqrt{F}(h-z)) + U_2 \sinh(\sqrt{F}(h+z))] - n \frac{G}{\mu F} \left[\frac{\cosh(\sqrt{F}z)}{\cosh(\sqrt{F}h)} - 1 \right] \quad (6)$$

$$v(z) = \frac{1}{\sinh(2\sqrt{F}h)} [V_1 \sinh(\sqrt{F}(h-z)) + V_2 \sinh(\sqrt{F}(h+z))] - n \frac{H}{\mu F} \left[\frac{\cosh(\sqrt{F}z)}{\cosh(\sqrt{F}h)} - 1 \right] \quad (7)$$

$$w \equiv 0, \quad p = -\rho g z - Gx - Hy + \varphi(t) \quad (8)$$

where $\varphi(t)$ is arbitrary time function.

In the case $\mathbf{V}_1 = \mathbf{V}_2$, the extreme values of velocity components are achieved at centerplane $z=0$ and are given by formulas

$$u_{\text{ext}} = \frac{U_1}{\cosh(\sqrt{F}h)} - n \frac{G}{\mu F} \left[\frac{1}{\cosh(\sqrt{F}h)} - 1 \right]$$

$$v_{\text{ext}} = \frac{V_1}{\cosh(\sqrt{F}h)} - n \frac{H}{\mu F} \left[\frac{1}{\cosh(\sqrt{F}h)} - 1 \right]$$

If $U_1 < nG/\mu F$, then, like in the classic case, the extreme value u_{ext} is the absolute maximum. If $U_1 > nG/\mu F$, then u_{ext} is the minimum value. Finally, if $U_1 = nG/\mu F$, then u -component is a constant function. The same is true for v -component with H substituted for G .

The important characteristic of the flow is the average velocity. For example, in x direction it can be evaluated for any height h as

$$Q = \frac{1}{2h} \int_{-h}^h u \, dz = \frac{U_1 + U_2}{2\sqrt{F}h} \tanh(\sqrt{F}h) - n \frac{G}{\mu F} \left[\frac{1}{\sqrt{F}h} \tanh(\sqrt{F}h) - 1 \right] \quad (9)$$

Similarly to the classic solution the generalized one can be obtained when the plates are inclined regarding vertical axis.

To compare these results with the classic ones, we present the horizontal velocity components and flow rate of the latter (the vertical component and pressure expressions are the same)

$$u_{\text{clas}} = \frac{G}{2\mu}(h^2 - z^2) + \frac{U_2 - U_1}{2h}z + \frac{U_2 + U_1}{2}, \quad v_{\text{clas}} = \frac{H}{2\mu}(h^2 - z^2) + \frac{V_2 - V_1}{2h}z + \frac{V_2 + V_1}{2} \quad (10)$$

$$Q_{\text{clas}} = \frac{U_1 + U_2}{2} + \frac{G}{\mu} \frac{h^2}{3} \quad (11)$$

One can demonstrate that the generalized solution approaches classic Couette–Poiseuille flow as n approaches 1 (that is, when porous medium disappears):

$$\lim_{F \rightarrow 0} u = u_{\text{clas}}, \quad \lim_{F \rightarrow 0} v = v_{\text{clas}}, \quad \lim_{F \rightarrow 0} Q = Q_{\text{clas}}$$

Let us consider two limit cases of the flow rate (9) with respect to the parameter h : the small height approximation ($h \ll 1$) and the great height approximation ($h \gg 1$). For small values of $\sqrt{F}h$ the following representation is valid:

$$Q = \frac{U_1 + U_2}{2} + n \left(\frac{G}{\mu} - F \frac{U_1 + U_2}{2} \right) \frac{h^2}{3} + O(F^2 h^4)$$

This expression reduces to the classic formula (11) as n approaches 1 (that is, when the porous medium disappears).

Also, direct calculation of limit as h approaches 0 in (9) and (11) yields

$$\lim_{h \rightarrow 0} Q = \lim_{h \rightarrow 0} Q_{\text{clas}} = \frac{U_1 + U_2}{2}$$

Therefore, when the influence of the boundaries (via no-slip boundary conditions) on the flow is strong or the porosity influence is negligible ($\sqrt{F}h \ll 1$) then the form of classic and generalized solutions is similar.

In the opposite limit of great height approximation ($h \gg 1$) we have a quite different situation. This is expected because in this case the flow is defined primarily by porous medium and the influence of far field boundaries is small (it can be neglected). The previous expression (11) holds for the classic solution, but the limit form of the average velocity of the generalized solution is

$$\lim_{h \rightarrow \infty} Q = n \frac{G}{\mu F}$$

Comparing the two expressions, we conclude that the limit of classic average velocity is infinity (if $G \neq 0$) as the height h becomes infinite, and, at the same time, the generalized solution approaches a constant value defined by pressure and gravitational force gradients in the flow direction. The last formula represents one of the forms of the experimental Darcy's law. The expression for permeability coefficient n/F was deduced analytically and calculated in the different regimes of flow by DuPlessis and Maslyiah [5].

Figures 2(a) and 2(b) show velocity profiles for different parameters of the problem. Figure 2(a) corresponds to the case of the equal boundary velocities and, consequently, the curves are symmetric with respect to $z = 0$ as it was indicated in previous analysis. For classic solution and generalized solution with weak porosity influence ($n = 0.9, F = 0.1$) the condition $U_1 < nG/\mu F$ is satisfied and both profiles have maximum value at $z = 0$. Other generalized solutions satisfy condition $U_1 > nG/\mu F$ and, in according with theoretical result, have minimum point at centerline. Figure 2(b) shows velocity profiles for asymmetrical case when boundary velocities are different. As it was expected, velocity values decrease crucially with increasing porosity terms in both cases. Presented curves for classic solutions can be compared with corresponding figures in well-known sources (for example, References [8, 9]).

The predicted behaviour of flow rate with respect to the height h can be observed in Figures 3(a) and 3(b), which present the flow rates for classic solution and three generalized

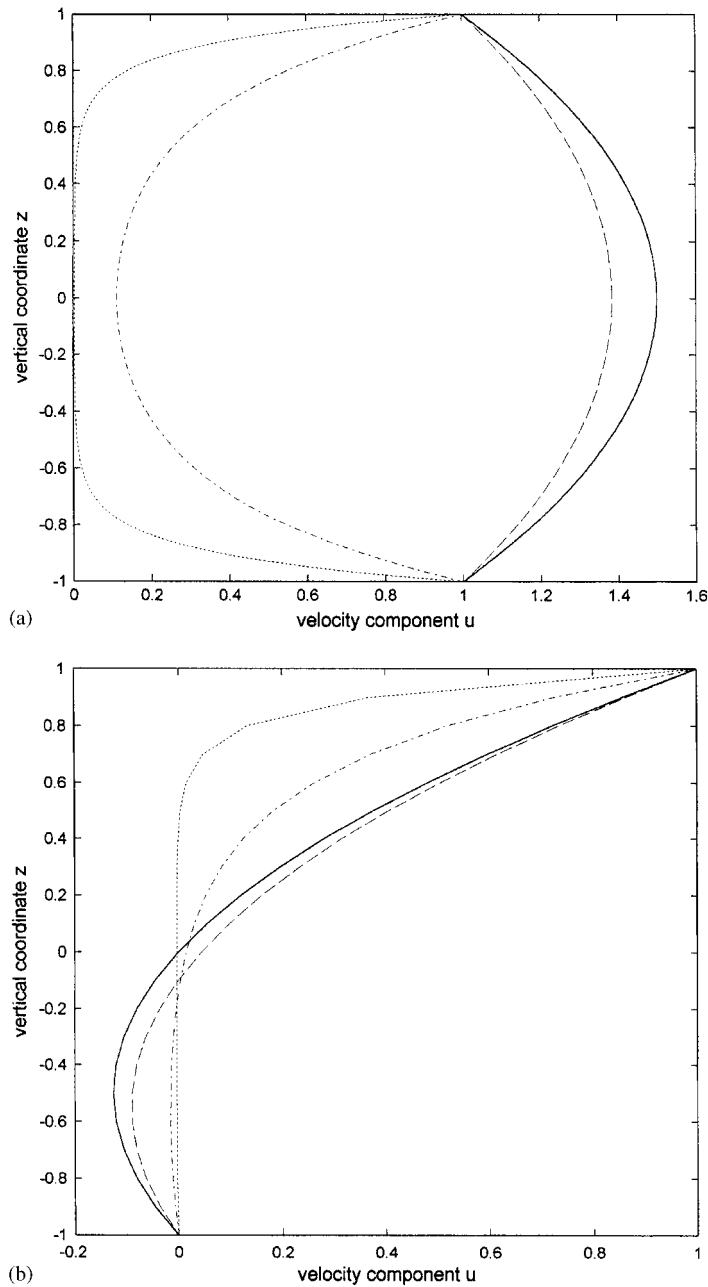


Figure 2. (a) Couette–Poiseuille flow: u -component profiles as a function of vertical coordinate z . Classic solution (solid curve) and three generalized solutions corresponding to $n=0.9$, $F=0.1$ (dashed curve), $n=0.3$, $F=10$ (dot-dashed curve) and $n=0.3$, $F=100$ (dotted curve) are plotted. Fixed problem parameters: $G=1$, $\mu=1$, $h=1$, $U_1=1$, $U_2=1$. (b) Same as in (a), except for $G=-1$, $U_1=0$, $U_2=1$.

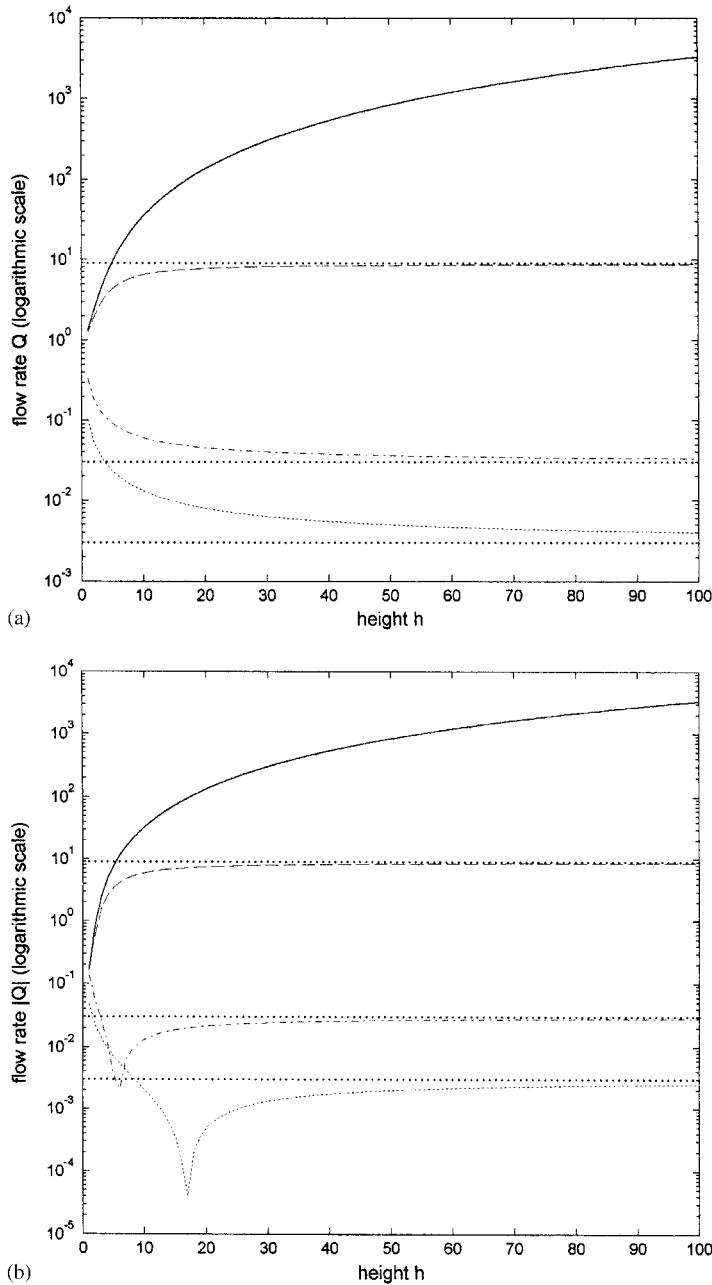


Figure 3. (a) Couette–Poiseuille flow: flow rate Q as a function of height h . Classic solution (solid curve) and three generalized solutions corresponding to $n = 0.9, F = 0.1$ (dashed curve), $n = 0.3, F = 10$ (dot–dashed curve) and $n = 0.3, F = 100$ (dotted curve) are plotted. Also Darcy’s flow rates are shown by separate point lines for indicated values of n and F . Fixed problem parameters: $G = 1, \mu = 1, U_1 = 1, U_2 = 1$. (b). Same as in (a) except for $|Q|$ and parameters $G = -1, U_1 = 0, U_2 = 1$.

solutions considered in Figures 2(a) and 2(b). In the small height approximation, the flow rates through porous medium are similar to classic flow and in the great height approximation they approach Darcy's law (separated point lines).

To use this solution for benchmarking purpose it is necessary to provide the respective differential problem in a bounded domain. This problem can be composed of Equation (1) in rectangular parallelepiped domain with boundary conditions (3) specified as follows:

$$\begin{aligned} w_{\Gamma} = 0, \quad u_{z=-h} = U_1, \quad u_{z=h} = U_2, \quad v_{z=-h} = V_1, \quad v_{z=h} = V_2 \\ u_{x=-a} = u_{x=a} = u_{y=-b} = u_{y=b} = u(z), \quad v_{x=-a} = v_{x=a} = v_{y=-b} = v_{y=b} = v(z) \end{aligned}$$

3. HAGEN-POISEUILLE FLOW

Now, let us derive the generalized Hagen-Poiseuille flow, i.e. fully established, axisymmetric steady flow of a viscous fluid through a straight round pipe of inside radius a located in a gravitational field (see Figure 4 for problem geometry). Choosing cylindrical co-ordinates r, θ, z where axis z coincides with centreline of the pipe and assuming velocity components in the form $v = 0, w = w(r)$, one can show that incompressibility equation together with homogeneous boundary conditions ($\mathbf{V}_{\Gamma} = 0$ in (3)) result in $u \equiv 0$ and other primitive equations yield the following decoupled equations

$$p_r = 0, \quad p_{\theta} = 0, \quad \mu \left(w_{rr} + \frac{1}{r} w_r - Fw \right) = -nG = np_z + n\rho g$$

where G is the separation constant. Then pressure is found with precision up to arbitrary constant B

$$p = -Gz - rgz + B$$

and axial velocity equation

$$w_{rr} + \frac{1}{r} w_r - Fw = -\frac{nG}{\mu} \quad (12)$$

can be transformed to a Bessel modified equation of order 0

$$x^2 \psi_{xx} + x \psi_x - x^2 \psi = 0 \quad (13)$$

by substitutions

$$x = \sqrt{Fr}, \quad \psi = w - \frac{n}{\mu F} G$$

The modified Bessel functions $I_0(x)$ and $K_0(x)$ are linearly independent solutions of Equation (13). Because $K_0(x)$ has a logarithmic singularity at the point $x=0$ then

$$\psi(x) = CI_0(x) = C \sum_{k=0}^{\infty} \frac{1}{(k!)^2} \left(\frac{x}{2}\right)^{2k}$$

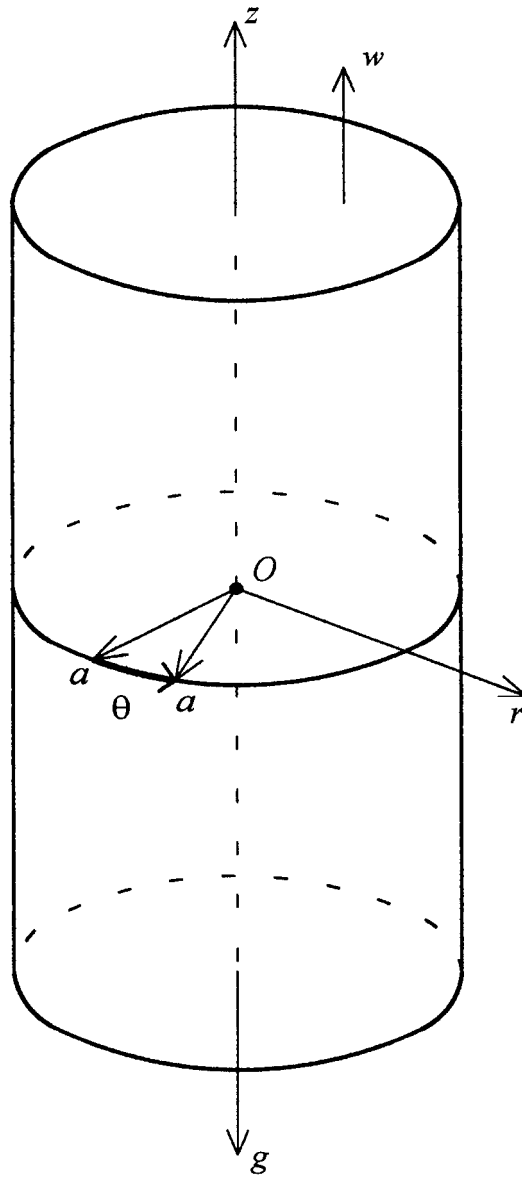


Figure 4. Geometry for Hagen–Poiseuille flow.

where C is constant. Therefore, a physically meaning solution of (12) is given as follows:

$$w(r) = CI_0(\sqrt{F}r) + n\frac{G}{\mu F} = C \sum_{k=0}^{\infty} \frac{F^k}{(k!)^2} \left(\frac{r}{2}\right)^{2k} + n\frac{G}{\mu F}$$

and C is defined from the homogeneous no-slip boundary condition through the formula

$$C \sum_{k=0}^{\infty} \frac{F^k}{(k!)^2} \left(\frac{a}{2}\right)^{2k} = -n \frac{G}{\mu F}$$

This solution can also be represented in the form

$$w(r) = -\frac{nG}{\mu F} \left[\frac{I_0(\sqrt{F}r)}{I_0(\sqrt{F}a)} - 1 \right] \quad (14)$$

Applying the ratio test one can prove a uniform convergence of the obtained series in any finite interval $[0, b]$. Then the flow rate

$$Q = \frac{1}{\pi a^2} \int_0^{2\pi} d\theta \int_0^a wr \, dr = \frac{2}{a^2} \int_0^a wr \, dr = -2 \frac{nG}{\mu F} \left[\frac{1}{a^2 I_0(\sqrt{F}a)} \int_0^a I_0(\sqrt{F}r)r \, dr - \frac{1}{2} \right] \quad (15)$$

can be calculated by integrating term by term the series in (14), leading to the following result:

$$Q = -\frac{2nG}{\mu F} \left[\frac{1}{I_0(\sqrt{F}a)} \sum_{k=0}^{\infty} \frac{F^k}{(k!)^2(2k+2)} \left(\frac{a}{2}\right)^{2k} - \frac{1}{2} \right] \quad (16)$$

For subsequent comparison, we present some elements of the classic solution:

$$w_{\text{clas}} = \frac{G}{4\mu}(a^2 - r^2), \quad Q_{\text{clas}} = \frac{Ga^2}{8\mu} = \frac{w_{\text{clas max}}}{2} \quad (17)$$

The results analogous to the Couette–Poiseuille flow approximations have been obtained for small and great radius approximations. In the case of $\sqrt{F}a \ll 1$, retaining the first two terms of the series in (14), we obtain the following approximation of the fourth order accuracy:

$$w(r) = n \frac{G}{\mu(4 + Fa^2)}(a^2 - r^2) + O(F^2 a^4)$$

When $n = 1$ this approximation coincides with classic solution.

As in the classic case, the maximum velocity is achieved at centreline $r = 0$ and has an expression

$$w_{\text{max}} = w(0) = -\frac{nG}{\mu F} \left[\frac{1}{I_0(\sqrt{F}a)} - 1 \right] = n \frac{Ga^2}{\mu(4 + Fa^2)} + O(F^2 a^4)$$

Relation (17) between flow rate and maximum velocity is not satisfied for generalized solution, but in small radius approximation it holds approximately:

$$Q = n \frac{Ga^2}{2\mu(4 + Fa^2)} + O(F^2 a^4) = \frac{w_{\text{max}}}{2} + O(F^2 a^4) \quad (18)$$

Comparing (18) with (17) one can observe that they have an equivalent form. The factor n has no qualitative influence and the term Fa^2 is sufficiently small in the small radius approximation. Therefore, when the influence of boundaries is strong or porosity is small then the form of classic and generalized solutions is similar.

When $a \gg 1$, i.e., boundaries have no practical influence on the flow rate, the behaviour of classic and generalized flows are quite different. It is difficult to prove a uniform convergence of the obtained series on the infinite interval $[0, +\infty)$ which is necessary for direct calculus of great radius limit in (16). Then, we use another method to evaluate the $\lim_{a \rightarrow \infty} Q(a)$. Let us denote

$$f(r) = I_0(\sqrt{F}r) = \sum_{k=0}^{\infty} \frac{F^k}{(k!)^2} \left(\frac{r}{2}\right)^{2k} \tag{19}$$

for brevity. It is evident, that partial sums of this series

$$s_n(r) = \sum_{k=0}^n \frac{F^k}{(k!)^2} \left(\frac{r}{2}\right)^{2k}$$

form the positive increasing sequence for any value of r . Then $s_n(r) < f(r)$ for any $n \in N$ and $\lim_{r \rightarrow \infty} f(r) = \infty$ because $\lim_{r \rightarrow \infty} s_n(r) = \infty$ for any n fixed. Therefore,

$$\lim_{a \rightarrow \infty} \int_0^a f(r)r \, dr = \infty$$

Now, considering the

$$\lim_{a \rightarrow \infty} \frac{\int_0^a f(r)r \, dr}{a^2 f(a)}$$

one can conclude that it represents an indeterminate form of type ∞/∞ . Since both numerator and denominator are continuously differential functions then the L'Hospital's rule can be applied:

$$\lim_{a \rightarrow \infty} \frac{\int_0^a f(r)r \, dr}{a^2 f(a)} = \lim_{a \rightarrow \infty} \frac{af(a)}{2af(a) + a^2 f'(a)} = \frac{1}{2 + \lim_{a \rightarrow \infty} (af'(a)/f(a))} \tag{20}$$

To calculate the limit in the right-hand side of (20) we observe that $\lim_{a \rightarrow \infty} f(a) = \infty$ and the derived series

$$\frac{1}{a} \sum_{k=1}^{\infty} \frac{F^k \cdot 2k}{(k!)^2 2^{2k}} a^{2k}, \quad F \sum_{k=0}^{\infty} \frac{F^k}{(k!)^2 2^{2k}} a^{2k}$$

converge uniformly in any finite interval. Then derivation term by term is allowed giving

$$g(a) = af'(a) = \sum_{k=1}^{\infty} \frac{F^k 2k}{(k!)^2 2^{2k}} a^{2k}, \quad \lim_{a \rightarrow \infty} g(a) = \infty$$

$$g'(a) = aF \sum_{k=1}^{\infty} \frac{F^{k-1}}{((k-1)!)^2 2^{2(k-1)}} a^{2(k-1)} = aF \sum_{k=0}^{\infty} \frac{F^k}{(k!)^2 2^{2k}} a^{2k} = aFf(a), \quad \lim_{a \rightarrow \infty} g'(a) = \infty$$

Therefore, the limit in the right-hand side of (20) is again an indeterminate form of type ∞/∞ and we can use the L'Hospital's rule twice to calculate this limit:

$$\begin{aligned}\lim_{a \rightarrow \infty} \frac{af'(a)}{f(a)} &= \lim_{a \rightarrow \infty} \frac{g'(a)}{f'(a)} = \lim_{a \rightarrow \infty} \frac{aFf(a)}{f'(a)} = \lim_{a \rightarrow \infty} \frac{a^2Ff(a)}{g(a)} = F \lim_{a \rightarrow \infty} \frac{2af(a) + a^2f'(a)}{g'(a)} \\ &= \lim_{a \rightarrow \infty} \frac{2af(a) + a^2f'(a)}{af(a)} = 2 + \lim_{a \rightarrow \infty} \frac{af'(a)}{f(a)}\end{aligned}$$

This is possible only when

$$\lim_{a \rightarrow \infty} \frac{af'(a)}{f(a)} = \infty$$

Consequently, the limit in left-hand side of (20) is equal to 0. Therefore,

$$\lim_{a \rightarrow \infty} Q(a) = \lim_{a \rightarrow \infty} 2 \frac{nG}{\mu F} \left[-\frac{1}{a^2 f(a)} \int_0^a r f(r) dr + \frac{1}{2} \right] = \frac{nG}{\mu F}$$

This signifies that the flow rate through the porous medium approaches Darcy's law when the boundaries are removed.

Obtained results are illustrated in Figures 5 and 6. Numerical calculations represented by plotted curves confirm the asymptotic behaviour of derived solutions for clear fluid and Darcy's porous flows.

To apply the obtained solution to a numerical simulation we derive the following rough estimate of series (19) remainder:

$$|R_n| \leq \frac{1}{(n+1)!} \exp \frac{Fr^2}{4}$$

Boundary conditions for benchmarking problem in a cylindrical domain can be formulated in the form:

$$u_\Gamma = 0, \quad v_\Gamma = 0, \quad w_{r=a} = 0, \quad w_{z=-c} = w_{z=c} = w(r)$$

4. STEADY UNIDIRECTIONAL FLOW THROUGH A RECTANGULAR CONDUIT

Let us consider a steady flow through a rectangular conduit in the direction of increasing x . To vary a physical model, we introduce the conduit inclined regarding gravitational axis (see Figure 7 for problem geometry). Using the problem simplifications $v \equiv 0$, $w \equiv 0$, $u_t = 0$ one can reduce Equations (1) to two separate equations

$$\mu(u_{yy} + u_{zz} - Fu) = -nG = np_x + n\rho g \sin \beta$$

Here β is the angle of inclination between x axis and the horizontal plane and G is the separation constant.

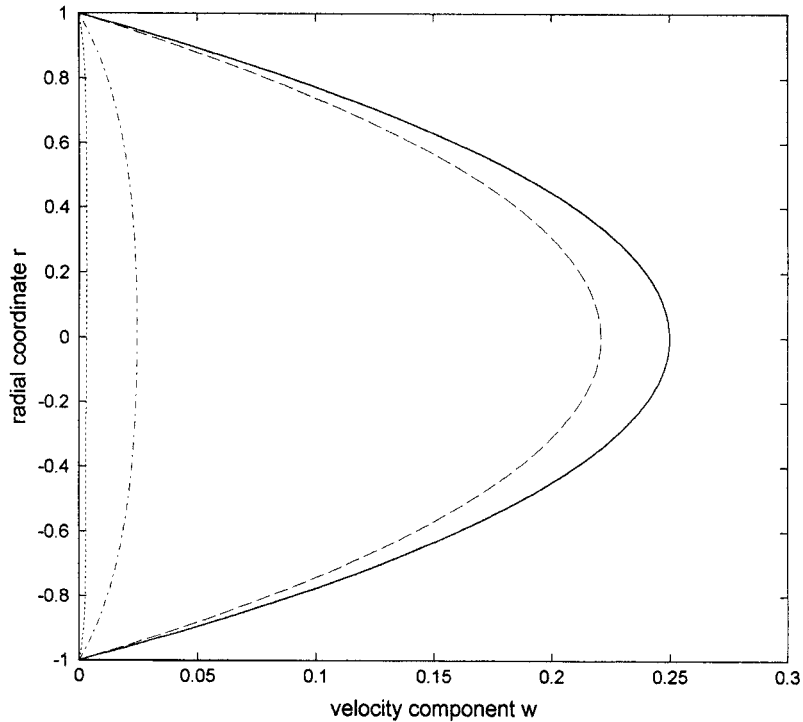


Figure 5. Hagen–Poiseuille flow: w -component profiles as a function of radial coordinate r . Classic solution (solid curve) and three generalized solutions corresponding to $n=0.9$, $F=0.1$ (dashed curve), $n=0.3$, $F=10$ (dot–dashed curve) and $n=0.3$, $F=100$ (dotted curve) are plotted. Fixed problem parameters: $G=1$, $\mu=1$, $a=1$.

Solution of Helmholtz equation

$$\mu(u_{yy} + u_{zz} - Fu) = -nG \tag{21}$$

subject to homogeneous boundary conditions

$$u(-b, z) = u(b, z) = 0, \quad u(y, -c) = u(y, c) = 0 \tag{22}$$

can be found as sum of two functions

$$u = \varphi + \psi$$

Here,

$$\varphi(z) = -n \frac{G}{\mu F} \left(\frac{\cosh \sqrt{F}z}{\cosh \sqrt{F}c} - 1 \right) \tag{23}$$

satisfies Equation (21) and homogeneous conditions with respect to variable z and ψ is the solution of the homogeneous equation

$$\psi_{yy} + \psi_{zz} - F\psi = 0$$

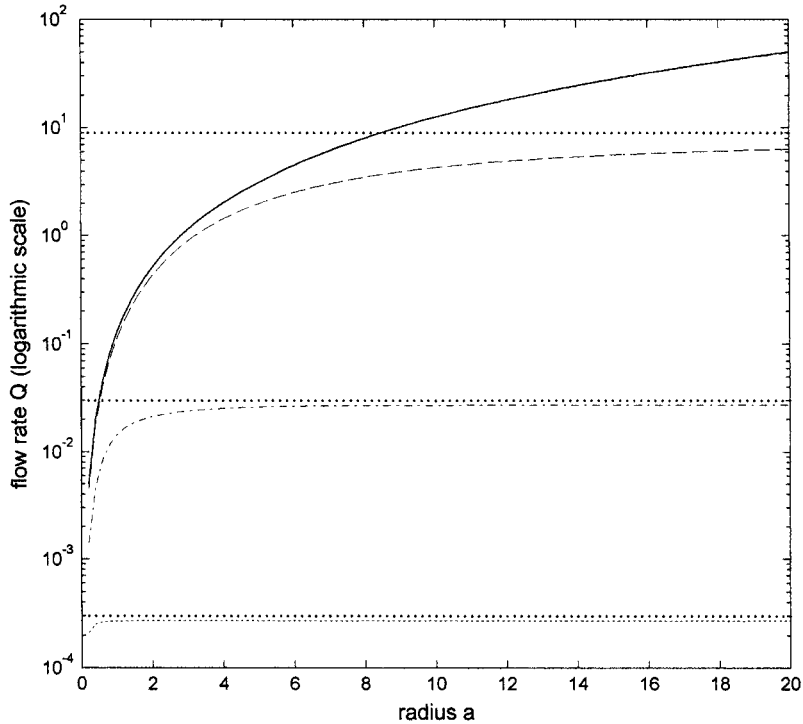


Figure 6. Hagen–Poiseuille flow: flow rate Q as a function of radius a . Classic solution (solid curve) and three generalized solutions corresponding to $n = 0.9, F = 0.1$ (dashed curve), $n = 0.3, F = 10$ (dot-dashed curve) and $n = 0.3, F = 100$ (dotted curve) are plotted. Also Darcy's flow rates are shown by separate point lines for indicated values of n and F . Fixed problem parameters: $G = 1, \mu = 1, a = 1$.

subject to the following boundary conditions:

$$\psi(y, -c) = \psi(y, c) = 0, \quad \psi(-b, z) = \psi(b, z) = -\varphi(z)$$

The last boundary value problem can be solved applying the method of separation of the variables. The solution has a form of series

$$\psi(y, z) = -n \frac{G}{\mu} \sum_{k=1}^{\infty} A_k \cosh \sqrt{F + \lambda_k} y \cos \sqrt{\lambda_k} z$$

where coefficients A_k are calculated by formulas

$$A_k \cosh \sqrt{F + \lambda_k} b \cdot c = \frac{2}{F + \lambda_k} \frac{1}{\sqrt{\lambda_k}} \sin \sqrt{\lambda_k} c, \quad \sqrt{\lambda_k} = \frac{2k - 1}{2c} \pi$$

Since obtained series is alternating one, the Leibnitz criteria can be applied to establish its uniform convergence.

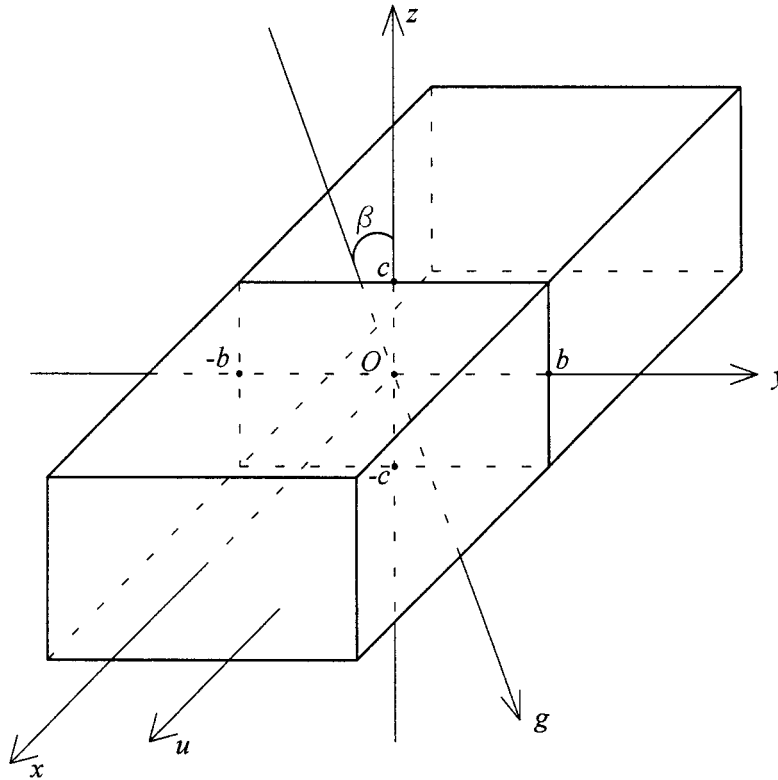


Figure 7. Geometry for rectangular conduit flow.

Finally, solution of problems (21) and (22) is obtained in the form

$$u(y, z) = -n \frac{G}{\mu F} \left(\frac{\cosh \sqrt{F} z}{\cosh \sqrt{F} c} - 1 \right) - n \frac{G}{\mu} \sum_{k=1}^{\infty} A_k \cosh \sqrt{F + \lambda_k} y \cos \sqrt{\lambda_k} z \quad (24)$$

The expression for pressure is given by formula

$$p = (G - \rho g \sin \beta)x - \rho g \cos \beta \cdot z + p_0$$

where p_0 is an arbitrary time function.

Some simple calculus demonstrate that this generalized solution approaches classic one

$$u_{\text{clas}}(x, y) = \frac{G}{2\mu} (z^2 - c^2) + \frac{G}{\mu} \sum_{k=1}^{\infty} B_k \cosh \sqrt{\lambda_k} y \cos \sqrt{\lambda_k} z$$

$$B_k \cosh \sqrt{\lambda_k} b \cdot c = \frac{1}{\sqrt{\lambda_k^3}} \sin \sqrt{\lambda_k} c$$

as n approaches 1.

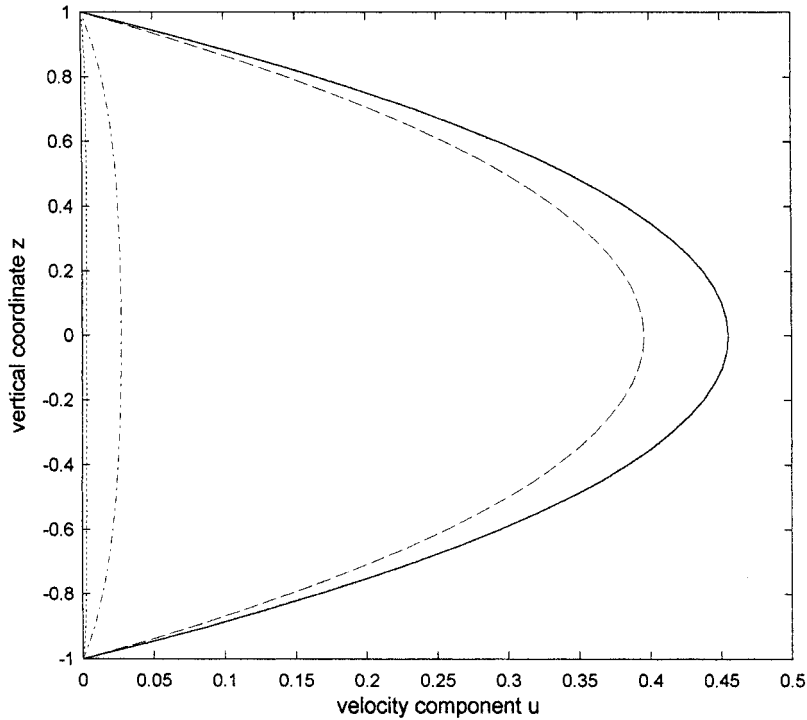


Figure 8. Rectangular conduit flow: profile of u -component as a function of vertical co-ordinate z along centreline $y=0$. Classic solution (solid curve) and three generalized solutions corresponding to $n=0.9$, $F=0.1$ (dashed curve), $n=0.3$, $F=10$ (dot-dashed curve) and $n=0.3$, $F=100$ (dotted curve) are plotted. Fixed problem parameters: $G=1$, $\mu=1$, $b=2$, $c=1$.

Due to uniform convergence series (21) can be integrated term by term and an expression for flow rate can be obtained for any conduit sizes:

$$Q = \frac{1}{4bc} \int_{-c}^c dz \int_{-b}^b u dy = -n \frac{G}{\mu F} \left[\frac{1}{\sqrt{F}c} \frac{\sinh \sqrt{F}c}{\cosh \sqrt{F}c} - 1 \right] - \frac{n}{\mu bc} \sum_{k=1}^{+\infty} \frac{A_k}{\sqrt{F + \lambda_k}} \frac{1}{\sqrt{\lambda_k}} \sinh \sqrt{F + \lambda_k} b \sin \sqrt{\lambda_k} c$$

Again the classic average velocity becomes infinite and flow rate through porous medium approaches Darcy’s law when the boundaries are removed:

$$\lim_{\substack{b \rightarrow \infty \\ c \rightarrow \infty}} Q(b, c) = n \frac{G}{\mu F}$$

The obtained results are illustrated in Figures 8–10. Figure 8 shows velocity component values along vertical line through geometric center of conduit and the Figures 9(a)–9(d)

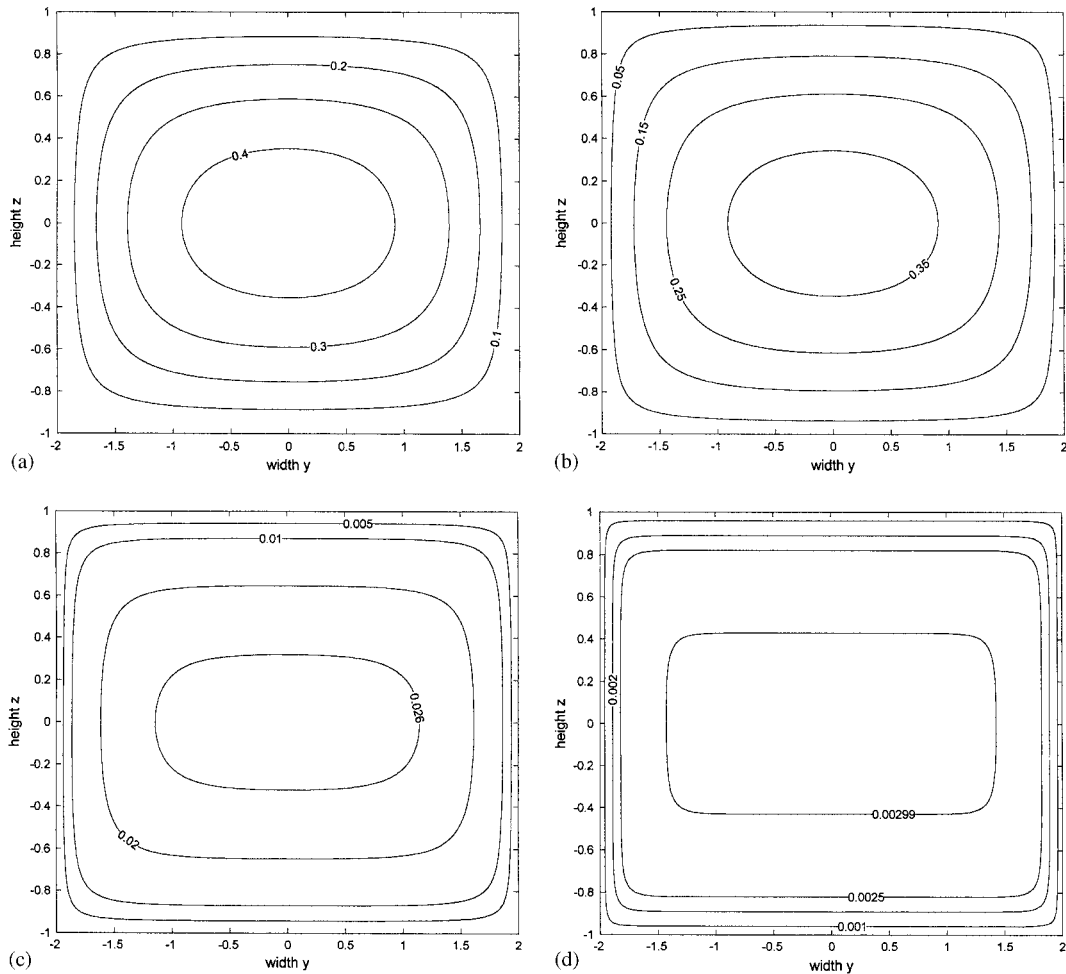


Figure 9. (a) Rectangular conduit flow: u -component contours. Classic solution for fixed problem parameters: $G=1$, $\mu=1$, $b=2$, $c=1$. (b) Same as in (a), except for generalized solution with $n=0.9$, $F=0.1$. (c) Same as in (a), except for generalized solution with $n=0.3$, $F=10$. (d) Same as in (a), except for generalized solution with $n=0.3$, $F=100$.

present some velocity contours for the same model problems. We use the same porosity parameters as in Figures 2 and 5. Again one can observe the effect of porous viscosity on the intensity of the flow. This influence can be even greater for natural porous media when n is varied from 0.3 for sand and gravel to 0.6 for some soils and values of F exceed 10^6 [10, 11]. The curve and contours for classic solution can be compared with corresponding figures in well-known sources (for example, References [8, 9]). Finally, in Figure 10, we show the flow rates corresponding to the velocity patterns presented in Figures (8), (9). Two asymptotic regimes of generalized solutions are clearly expressed by plotted curves.

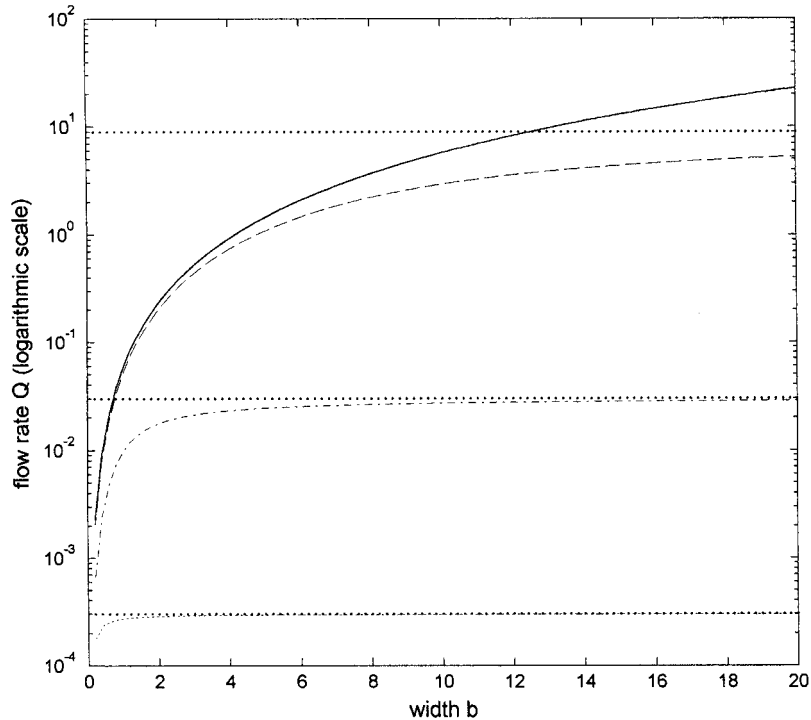


Figure 10. Rectangular conduit flow: flow rate Q as a function of width b . Classic solution (solid curve) and three generalized solutions corresponding to $n=0.9$, $F=0.1$ (dashed curve), $n=0.3$, $F=10$ (dot-dashed curve) and $n=0.3$, $F=100$ (dotted curve) are plotted. Also Darcy's flow rates are shown by separate point lines for indicated values of n and F . Fixed problem parameters: $G=1$, $\mu=1$, $c=b/2$.

To apply obtained solution to numerical simulation we have to formulate the differential problem in limited domain and evaluate the partial sums of series. To evaluate the partial sums we used Leibnitz criteria again and established required remainder estimate:

$$|R_n| \leq \frac{c^2}{(n+0.5)^3 \pi^3}$$

The required benchmarking problem can be done in the form of Equation (1) in Cartesian co-ordinates with the boundary conditions

$$v_\Gamma = 0, \quad w_\Gamma = 0, \quad u_{y=-b} = u_{y=b} = u_{z=-c} = u_{z=c} = 0, \quad u_{x=-a} = u_{x=a} = u(y, z)$$

We observe that in the case of moved z -boundaries with velocities (23) the solution (24) reduces to the only term $\varphi(z)$ and, consequently, takes the simplest form. Analogous observation is valid for moved y -boundaries.

5. CONCLUSIONS

Some exact solutions of the generalized Navier–Stokes equations describing incompressible flows in a porous media are derived. The evaluation of small porosity and close boundaries regimes showed proximity of these solutions to classic ones. In the case of removed boundaries, obtained solutions approximate flows governing by Darcy’s law. Based on the derived analytical solutions, the benchmarking problems in bounded domains are formulated. The exact solutions are for standard planar and axisymmetric geometries and can be used to benchmark various numerical schemes that use this equation set.

ACKNOWLEDGEMENTS

Author is grateful to anonymous reviewer for many useful comments that permitted to improve the text. Author is also grateful to Lioudmila Bourchtein for useful discussions and to Paola Jaekel for preparing the figures. This work was supported in part by Brazilian Foundation FAPERGS under grant 01/60053.9.

REFERENCES

1. Wang CY. Exact solutions of the unsteady Navier–Stokes equations. *Applied Mechanics Review* 1989; **42**: 269–282.
2. Wang CY. Exact solutions of the steady-state Navier–Stokes equations. *Annual Reviews of Fluid Mechanics* 1991; **23**:159–177.
3. Brinkman HC. A calculation of the viscous force exerted by a flowing fluid on a dense swarm of particles. *Applied Scientific Research* 1947; **A1**:27–34.
4. Hinch EJ. An averaged equation approach to particle interactions in a fluid suspension. *Journal of Fluid Mechanics* 1977; **83**:695–720.
5. DuPlessis PJ, Masliyah JH. Flow through isotropic granular porous media. *Transport in Porous Media* 1991; **6**:207–221.
6. Constantin P, Foias C. *Navier–Stokes Equations*. University of Chicago Press: Chicago, 1989; 190.
7. Gresho PM. Incompressible fluid dynamics: some fundamental formulation issues. *Annual Reviews of Fluid Mechanics* 1991; **23**:413–453.
8. Granger RA. *Fluid Mechanics*. Dover Publications: New York, 1995; 896.
9. Yih C-S. *Fluid Mechanics*. McGraw-Hill: New York, 1977; 622.
10. Bird RB, Stewart WE, Lightfoot EN. *Transport Phenomena*. Wiley: New York, 1960; 808.
11. Bear J. *Dynamics of Fluids in Porous Media*. Dover Publications: New York, 1988; 764.